Journal of Energy Storage 96 (2024) 112665

Contents lists available at ScienceDirect

Journal of Energy Storage

journal homepage: www.elsevier.com/locate/est

Research papers

Properties of $AlCl_3$ guanidine deep eutectic solvent with addition of polyethylene oxide of different molecular weights supported by quantum-chemical calculation

Roman Tangalychev [a,*,1], Vasilii Korotenko [b,1], Igor Efimov [c], Oleg N. Efimov [d]

[a] Technische Universität Ilmenau, Institute for Automation and Systems Engineering, Department of Computer Science and Automation, Ehrenbergstraße 29, 98693 Ilmenau, Germany
[b] Forschungszentrum Jülich GmbH, Institute of Energy and Climate Research (IEK), Fundamental Electrochemistry (IEK-9), Wilhelm-Johnen-Straße 802, 52428 Jülich, Germany
[c] The University of Sheffield, Department of Chemical and Biological Engineering, Mappin Street, Sheffield S1 3JD, United Kingdom
[d] Federal Research Center of Problems of Chemical Physics and Medicine Chemistry, Russian Academy of Sciences, 142432 Chernogolovka, Moscow region, Russian Federation

ARTICLE INFO

Keywords:
Deep eutectic solvents
Electrochemical aluminum deposition
Macromolecules polyethylene glycols
DFT
DLPNO-CCSD(T)
Voltammetric analysis

ABSTRACT

Deep eutectic solvent of $AlCl_3$ with guanidine HCl was synthesized in the molar ratio 3:1 in the presence of polyethylene glycols of various molecular weights from 1500 to $5{\cdot}10^6$ g/mol. Concentration of polymer was 2.5 %, 5 % and 10 %. Temperature dependence between 25 and 70 °C of conductivity of each electrolyte was calculated from the cyclic voltammetry of aluminum deposition-stripping measurements. It was found that conductivity increases with molecular weight of polymer in the interval between 2 and 10 kD. This result was interpreted as binding of $AlCl_3$ guanidine to two different sites which have hydroxyl (chain ends) and ether (middle chain) oxygen with relatively higher and lower binding energy respectively. Polymer with longer chain has more low energy binding sites which causes lesser binding and consequently higher conductivity of electrolyte. B3LYP-D3 and DLPNO-CCSD(T) computations support experimental results. DES are discussed in terms of Pearson HSAB principle.

1. Introduction

Rechargeable batteries have become important as carbon dioxide emission free power sources for electrical vehicles and other applications. However, Li based as they are almost exclusively now, they have critical disadvantages as flammability and scarcity of cathode materials, which necessitates their costly not environmentally friendly recycling. In other words, they are not cheap, and not "green". So, Li batteries are not exactly fit to the purpose they were introduced from start, which is reflected by recent decrease of EV market.

In view of the above, a number of scientific groups are investigating the possibility of using other metals (Na, K, Mg, Ca, Zn and Al, etc.) in the production of the rechargeable batteries [1]. From mass per exchanging electron, one can immediately conclude that it is Al^{3+} (27/3 = 9 g/mol) which is the closest suitable ion to replace Li^+ (6.9 g/mol).

Chemical current sources based on aluminum have a number of qualitative advantages. The main one is the electrical capacity of aluminum batteries (8000 mAh*cm^3 vs 2000 mAh*cm^3 for Li-ion). Aluminum is present in the earth's crust in a larger amount when compared to lithium (8 % Al compared to <0.01 % Li). The distinctive parameters of an aluminum-ion battery are: short charging time (less than one minute at a current density of 4000 mA/m^2) and durability (6000–7500 charge-discharge cycles) [2–5]. In addition, it is known that the features of electrochemical processes in aluminum-based electrolytes do not allow the formation and growth of dendrites on the electrodes, which prevents a possible short circuit in the device. It is worth noting that to create this type of battery, it is necessary to use anhydrous electrolytes that can create conditions for a multiple process of dissolution and intercalation of aluminum in the structural parts of a chemical current source.

Successful tests were performed in an electrolyte based on imidazolium and pyrrolidinium chloride ionic liquids, (1-ethyl-3-

* Corresponding author.
E-mail address: roman.tangalychev@tu-ilmenau.de (R. Tangalychev).
[1] These authors contributed equally to this work.

https://doi.org/10.1016/j.est.2024.112665
Received 8 February 2024; Received in revised form 25 May 2024; Accepted 16 June 2024
Available online 25 June 2024

methylimidazolium chloride, [EMIm]Cl [3,6,7], and 1-butyl-3-methylimidazolium chloride [BMIM]Cl) and other imidazoliums, mixed with aluminum chloride ($AlCl_3$) [8], in carbamide (urea) with $AlCl_3$ [9], in various amides with $AlCl_3$ [10], and in triethylammonium chloride (Et_3NHCl) with $AlCl_3$ ionic liquids [11].

Recently new chloroaluminate DES have been proposed [12] based on Pearson HSAB, Hard and Soft Acids and Bases principle [13]. $AlCl_3$ is typical "hard Lewis acid". It is defined by low polarizability and large charge. According to HSAB it binds preferably to Lewis base with the same properties. All Lewis bases studied so far were soft bases imidazoliums or urea. It was proposed that hard bases should be tried. Because of their ionic character, they should be searched within Lewis bases with high melting temperature. The following bases have been found acetamidine HCl, guanidine HCl and BMP Cl. They have melting temperatures above 180 °C. Which makes them different from imidazoliums with extended π system and Tm = 60–70 °C, or urea Tm = 110 °C.

During battery discharge, Al^{3+} binds into stronger ionic compound in DES, thus the final state has lower energy and the current increases.

This paper proceeds with investigation of anodic half reaction from AlCl3 guanidine DES in different polymer solutions. They are expected to stabilize electrolyte, since it consists of the strongest Lewis acid and base and prone to precipitation and thickening. The results can be useful for electrochemical deposition of Al on its own. Sine cathodic half reaction is entirely different subject, it is not touched here, and full cell as well. However, one can say that graphite cathode with pvdf/nmp or sodium alginate binders works with this DES but needs improvement. Acetamidine and guanidine batteries were recently reported [5,14].

Polyethyleneoxide/-glycol (PEO, or PEG) of 100–5000 kD molecular weight was found to mix surprisingly well with chloroaluminates ionic liquids, as AlCl3 EMIM Cl, or AlCl3 Urea [15–18] as well as acetamidine (also polyamide [5]), guanidine and BMP Cl (unpublished data). Experiment is straightforward: the dry polymer is added either to synthesis batch or to ready DES and heated to 80-90C. The resulting plastic is conductive and can be exposed to air. Therefore, it is useful for batteries construction. It was found that shorter chains <100 kD do not produce smooth gel. This puzzling observation is the topic of current paper.

In this work, the effect of additives of PEG polymer macromolecules (PEG–1500; PEG–2000; PEG-CH_3–2000; PEG–4000; PEG–9000; PEG–20000; PEG–5 million) on the process of electrochemical deposition-dissolution of aluminum as a function on the temperature of the electrolyte was studied. Polymers were added to the system in mass concentrations from 2.5 % to 10 %, which, together with obtaining results on the temperature effect on voltage and current density, allowed us to find Activation Energy values (E_a) for each electrochemical system. Fittings were created to build diagrams reflecting the results of the process. In the course of experimental studies, after obtaining laboratory results, during analytical processing it is planned in this article to apply the ionic conductivity equation to create fittings and plot graphs and curves of the activation energy dependences on molecular weight. The equation describes a mathematical model of the process and has been tested in a number of studies and has repeatedly confirmed its effectiveness [12,15,19].

2. Materials

All reagents used in this study are chemicals with an analytical degree of purity. Polyethylene glycol (PEG) with different molecular weights (M_n = 1500 – 5mln g/mol) was produced and supplied by Sigma Aldrich, BASF and Thermoscientific, respectively. Guanidine hydrochloride/GuanHCl (CH_5N_3–HCl) 98 % was purchased by Alfa Aesar. Aluminum chloride ($AlCl_3$) was purchased from Q-BASF. All reagents were used without additional purification. Melts of samples-electrolytes of amidine solutions were compiled and used immediately for experimental purposes. Aluminum anode CA–III-B (Al-Zn-Si, B-) containing tin (Sn) 5.5–7.0 %, boron (B) 0.025–0.035 %, silicon (Si) 0.1–0.15 %, iron (Fe) 0.09 % and 0.006 % copper (Cu) were used as elements of the galvanic cell; pure copper and brass were used as cathodes and an aluminum wire as reference electrode.

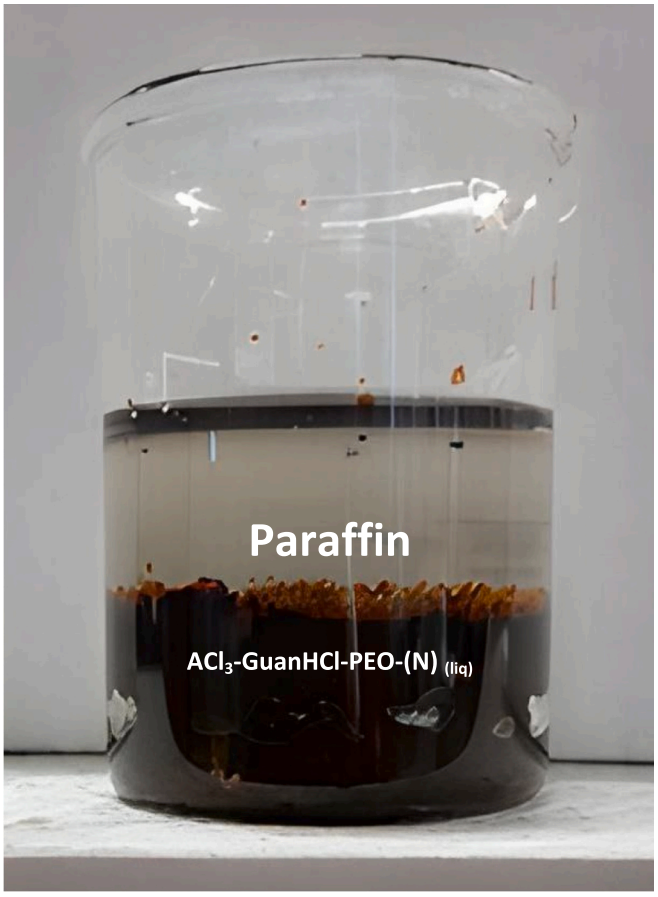

Fig. 1. A typical $AlCl_3$ guanidine HCl DES.

3. Methodology

To conduct an experiment to determine the activation energy and identify the phase transition in the GuanHCl – $AlCl_3$ – polymer system (Fig. 1), a number of electrolyte solutions with a molar ratio of GuanHCl: $AlCl_3$ = 1:3 was compiled. That was based on the successful results in previous study [12], however the ratio was increased to assure that AlCl3 during heating is always in saturating concentrations. The analyzed amounts of polymers were added, from 2.5 to 10 wt%. The used experimental procedure was as following: Selection of a container for mixing reagents and filling it with 10 % of the volume of a hydrocarbon in liquid form [12] to create an insulating film on the surface of the system. The procedure was run on bench, not in glove box, therefore isolation from air and humidity was necessary. The hydrocarbon also provided better contact and heat exchange between solid reactants. The calculated masses of reagents are introduced into the container alternately, first aluminum chloride, then GuanHCl, and at the end – a certain mass of polymer.

1. The mixing process begins in parallel to local heating, which was applied from an external source (heating tile or heat gun), in order to dissolve the reagents and to obtain a homogeneous viscous liquid.
2. When the critical temperature of dissolution of the reagents in the system is reached, a transition occurs to the termination of the heat supply and the continuation of mixing until a homogeneous consistency in the solution;

3. Separation of the solution from the liquid hydrocarbon with an extraction glass-pipette;
4. Assembling an electrochemical cell (aluminum anode, aluminum reference electrode and copper cathode); some layer of aforementioned hydrocarbon always remained on top, since it had lower density. It was well separated and allowed to run experiments on bench, not in glovebox, without altering the data [20].
5. Electrolyte introduced into the cell (approximately 20 ml) and contacting the electrodes to a BioLogic SP150 potentiostat;
6. Conducting all experimental processes on EC-Lab V11.30 and recording cyclic voltammograms (CV) of the studied electrolytes in the temperature range from 25 °C to 70 °C. The cathodic current, which corresponds to the process of aluminum deposition, and the anodic peak, which characterizes the dissolution of aluminum on the cathode surface, have been analyzed.

An exponential equation was used for fitting the current density and potential recorded during the anodic scan (Eq. (1)). The activation energy of electrolytes based on their composition and temperature was thus calculated.

4. Computational methodology

Quantum-chemical computations were employed to assess the gas-phase enthalpy (H^{gas}) and Gibbs free energy (G^{gas}) of non-covalent intermolecular interactions formation. (The superscript ^{gas} denotes a gas phase standard state at 298.15 K and 1 atm.) Namely, such an analysis was carried out for the formation reaction of the Guan-$AlCl_3$ dimer and the Urea-$AlCl_3$ dimer (Table 2). Additionally, we use the reaction of trimer formation from a Guan-AlCl3 complex and one small molecule (oligomer) as a model to evaluate non-covalent intermolecular interactions between the Guan-$AlCl_3$ complex and the PEG polymer. As an oligomer simulating functional groups and fragments of the macromolecules of the PEG polymer, we are testing compounds such as ethanol, ethylene glycol, dimethyl ether, 1,2-dimethoxyethane (Table 3). Ethanol and ethylene glycol molecules model the terminal parts of the PEG polymer, while dimethyl ether and 1,2-dimethoxyethane describe its internal portions.

DFT calculations were performed using Gaussian09, Revision D.01 [21]. An initial 100 structures were randomly generated for each of the molecular complexes modeled in this work using the «kick» algorithm [22,23]. Geometry optimizations have been performed using the B3LYP hybrid functional [24,25] complemented by the D3 dispersion correction [26]. The 6-31+G(d,p) all electron basis set have been used for all elements [27]. Frequency calculations have been carried out to verify that the optimized structures are true minima. Thermochemical corrections to H^{gas} and G^{gas} were calculated using the entropic quasi-harmonic treatment with frequency cut-off value of 100.0 wavenumbers [28]. The individuality of the found conformers was confirmed using an energy criterion $\Delta E_{tot} > 10^{-7}$ Hartree and comparing geometries by distances between each atom and the centroid point [29–31]. Following previous studies on organometallic compounds [32–34], we performed single point B3LYP-D3 calculations for found conformers with a more extended basis set 6-311++G(2df,2p) to analyze the DFT energies in Tables 2 and 3. Additionally, single point energies have subsequently been calculated with the DLPNO-CCSD(T) method [35,36] as implemented in ORCA 5.0.4 [37] in combination with the cc-pVTZ and cc-pVQZ basis sets, followed by extrapolation to the complete basis set (CBS) limit to DLPNO-CCSD(T)/CBS total energies [35,38]. Enthalpies and free energies at 298.15 K have then been obtained through combination of the single point total energies with thermochemical corrections calculated at the B3LYP-D3/6-31+G(d,p) level before.

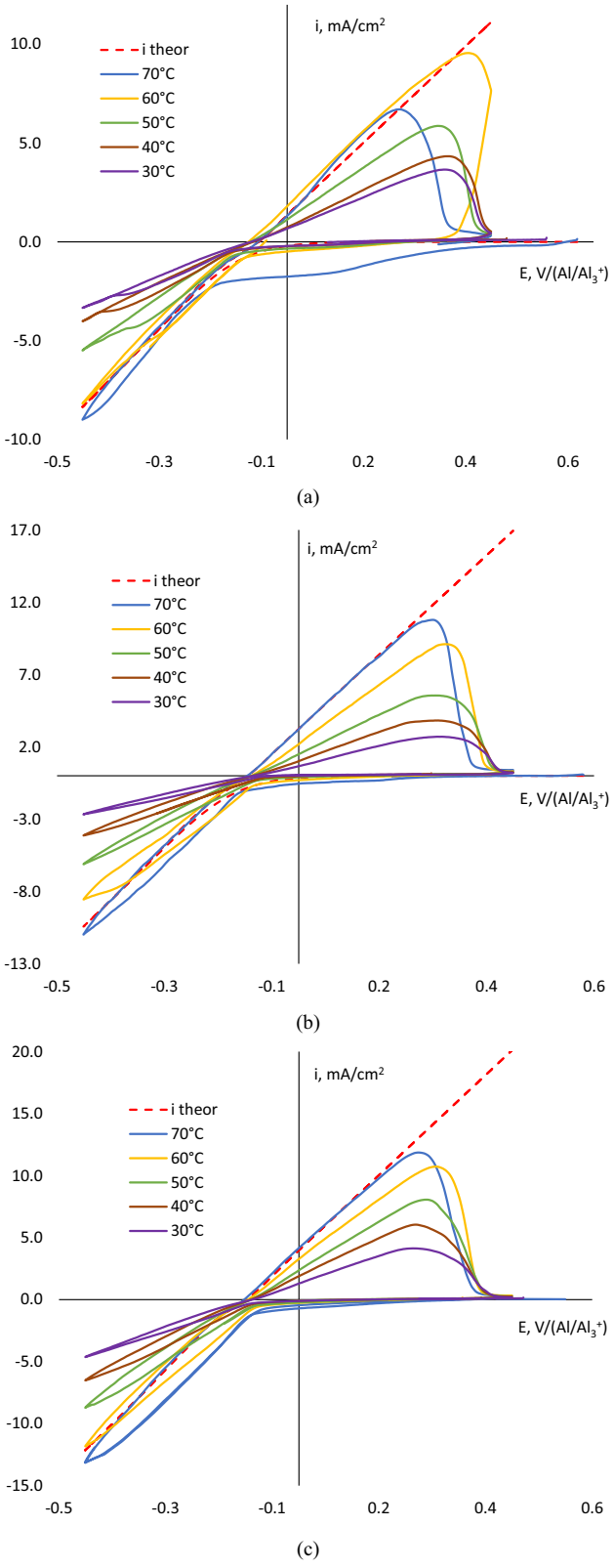

Fig. 2. Typical experimentally obtained cyclic voltammetry at different temperatures and its corresponding calculated theoretical approximation (red line) for **(a)** GuanHCl – $AlCl_3$ – PEG-5million(kk) (5 % w/w); **(b)** GuanHCl – $AlCl_3$ – PEG$(CH_3)_2$-2000 (5 % w/w); **(c)** GuanHCl – $AlCl_3$ – PEG-9000 (5 % w/w). Scan rate = 20 mV/s. (For interpretation of the references to color in this figure legend, the reader is referred to the web version of this article.)

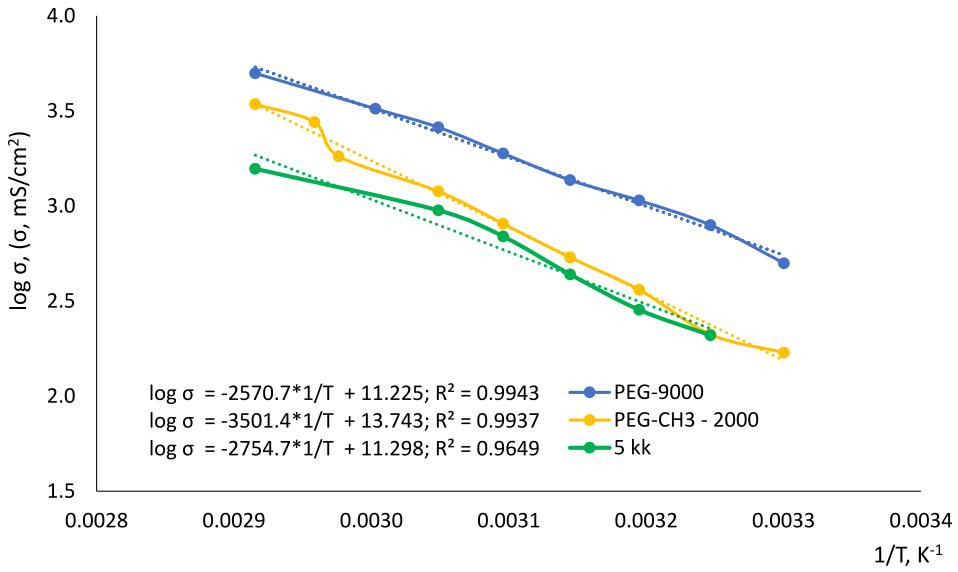

Fig. 3. A typical Arrhenius dependence of logarithm ionic conductivity on inverse temperature. The concentration of polymers is 5 % (w/w).

5. Experimental part

The experiments were carried out in the temperature range from 70°C to 30 °C, the cooling occurring under normal conditions. Cyclic voltammograms were recorded at a scan rate of 20 mV/s in the voltage range from −0.4 V to +0.4 V vs Al/Al^{3+} RE. The step of recording the indicators was set to 5 °C. In addition, the physical properties of the electrolyte (color, viscosity) were qualitatively noticed. The cathode plate was investigated by bare eyes after the deposition was completed, in order to see if metal deposition (aluminum) occurred on it, the quality and color of the deposit, and in rare cases, its thickness. This inspection was of interest in terms of identifying the effect of added polymer molecules in the electrolyte. PEG could act as structuring agents for the electrolyte, as well as additives in the near-electrode region during the diffusion of aluminum compounds to/from the electrical double layer.

A fitting on the experimentally obtained current densities and potential curves was performed with MS Excel program (with a pre-installed Solver package) according to Eq. (1) and also used the logarithm of pre-exponent equation of ionic conductivity, compiled to solve similar problems [15]:

$$i = \frac{\sigma\varphi i_0\left(exp\left(\frac{nF(1-\alpha)\varphi}{RT}\right) - exp\left(\frac{-nF\alpha\varphi}{RT}\right)\right)}{\sigma\varphi + i_0\left(exp\left(\frac{nF(1-\alpha)\varphi}{RT}\right) - exp\left(\frac{-nF\alpha\varphi}{RT}\right)\right)} \quad (1)$$

where R – universal gas constant, F - Faraday constant, T - temperature, n (=3) – the number of electrons, $\varphi = E\text{-}E_0$ – potential with respect to potential of zero current E_0, σ - electrical conductivity, α – transfer coefficient.

The obtained current density values were compared according to the composition of the electrolyte, in particularly, to the polymer macromolecules added in the solution (with molecular weight from 1500 to 5 million). When recording the values from the potentiostat, the step was determined by the temperature value and was a difference of 10 °C, which made it possible to apply the Arrhenius law to the presented systems.

A typical graph for the experimental obtained data and the data obtained by the fitting with Eq. (1) is shown in Fig. 2.

As it can be seen from the Fig. 2, the experimentally obtained data are in agreement with the theoretical assumption formed by the mathematical fitting model for the cathodic sweep. The activation energy (E_a) values predicted by the Arrhenius equation Eq. (2) reflect the studied values for each GuanHCl – $AlCl_3$ – Polymer system in a given voltage range.

Table 1
The E_a, R^2 (correlation factor) and *log k* (logarithm of pre-exponent) values calculated for the system GuanHCl:$AlCl_3$ = 1:3 from the cyclic voltammograms experiments; dE/dt = 20 mV/s. A copper cathode (56 mm^2 geometrical area) was used.

System GuanHCl-$AlCl_3$	E_a, kJ/mol	R^2	log k
Without additive of the polymer	18.7	0.98	10.1
+2.5 % PEG–1500	28.8	0.97	14.6
+2.5 % PEG–4000	21.0	0.98	11.5
+2.5 % PEG–5 million	22.0	0.96	11.3
+2.5 % PEG-$(CH_3)_2$–2000	28.0	0.99	13.8
+2.5 % PEG–9000	20.6	0.99	11.2
+5 % PEG–9000	24.8	0.99	12.0
+5 % PEG–20000	26.4	0.98	13.3
+5 % PEG–2000	33.5	0.95	16.2
+5 % PEG-$(CH_3)_2$–2000	20.6	0.98	11.7
+5 % PEG–4000	22.6	0.96	12.5
+5 % PEG–1500	31.7	0.90	14.8
+5 % PEG–5 million	41.5	0.99	18.4
+10 % PEG–2000	27.3	0.99	12.5
+10 % PEG–1500	25.5	0.99	11.9
+10 % PEG–20000	35.3	0.97	15.5
+10 % PEG-$(CH_3)_2$–2000	28.6	0.98	13.3
+10 % PEG–9000	30.4	0.99	14.3

$$\sigma = k\, e^{-\frac{E_a}{RT}}; \quad (2)$$

The value of the activation energy (E_a) for each system in the specified temperature range was determined from graphical representation of the temperature dependence of the ionic conductivity. Such a curve used to calculate the E_a values is shown in Fig. 3.

Fig. 3 shows an Arrhenius dependence curve of the GuanHCl-$AlCl_3$ system with polymers PEG-9000, PEG-5million(kk) and PEG-$(CH_3)_2$ with a molecular weight of 2000 and a specific concentration of polymer in the system of 5 %. All experimental and computational studies of all types of electrolytes investigated here are summarized in Table 1.

As it can be seen from the Table 1, the obtained activation energy values (E_a) have a high calculated accuracy, based on $R \geq 0.95$ (except for the experiment with PEG-20000 2.5 % weight.). All this confirm the assumption that the introduction of a polymer as additive into the ionic liquid electrolyte qualitatively affects the ionic conductivity.

The calculated activation energies (E_a) as a function of the

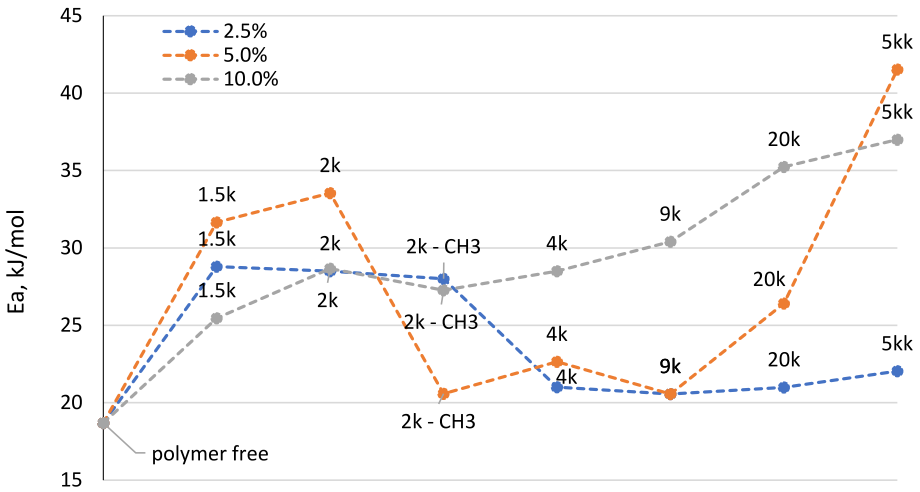

Fig. 4. The graphical representation of the E_a as a function of the molecular weight of the PEG molecule and its amount added in the system GuanHCl:$AlCl_3$ = 1:3; dE/dt = 20 mV/s; a copper cathode (56 mm^2 geometrical area).
*k – 1000, kk – million (the molecular weight);
** The vertical line on the right side of the Fig. indicates a gap that separates points with a high polymer molecular weight.

composition of the electrolytes are illustrated in Fig. 4.

6. Model for binding and dependence on polymer length

The data in Fig. 4 can be explained using a statistical model. As shown above, there are two types of binding sites of GuanHCl-$AlCl_3$ on polymer: on the ending, hydroxyl groups and in the inner "middle" ether sites. Let the binding energy be E_{end} and E_{mid} respectively. Then, for the polymer consisting of N units: $N = M/44$, where M is polymer molecular mass, and 44 g/mol is the mass of a single unit. Each unit is equivalent binding site with energy E_{mid}. The same will be activation energy for leaving the site. Two ending sites have binding and activation energies for leaving E_{end}. The following equation applies for the effective binding energy E_{eff}, which is also activation energy measured in the experiment: (Eq. (3))

$$(N+2)exp\left(\frac{E_{eff}}{RT}\right) = 2exp\left(\frac{E_{end}}{RT}\right) + Nexp\left(\frac{E_{mid}}{RT}\right) \quad (3)$$

This leads to equation for effective activation energy at $N \gg 1$: (Eq. (4))

$$E_{eff} = RTln\left(\frac{2}{N}exp\left(\frac{E_{end}}{RT}\right) + exp\left(\frac{E_{mid}}{RT}\right)\right) \quad (4)$$

which provides dependence on polymer length N in terms of binding energies on 2 types of sites. This equation can be directly compared with Fig. 4 data. Fitting to 2.5 concentration data gives 34.4, 21.9 kJ/mol for E_{end} and E_{mid} respectively. For 5 % concentration 37.9, 24.0 kJ/mol for E_{end} and E_{mid}. 10 % solutions already exhibit viscous behavior and do not obey this model. The values obtained are quite far from those provided in quantum chemical calculations. This difference stems from the simplified molecular structures used in the quantum chemical calculations. Also, DFT and CBS calculation access thermodynamic values, whereas conductivity activation energy is a kinetic parameter. Though on would expect that stronger binding implies escape higher barrier, as follows from linear relation of free energies principle.

7. Computational results

The use of enthalpy (ΔH^{gas}) or Gibbs free energy (ΔG^{gas}) for comparison is not an obvious point in this study. On the one hand, the use of Gibbs free energy (ΔG^{gas}) values for comparison are justified by the fact that the coupling constant between molecules is the logarithm of free energy, therefore the entropy factor is considered. On the other hand, the computational model used in the study for DFT is intentionally reduced to a chain of a few atoms (functional radicals). In view of this, the entropy factor, which directly depends on the number of atoms, will have incorrect values. At the same time, the values when comparing the enthalpy will have a smaller error (based on the given model), since the

Table 2
The calculated Boltzmann averaged ΔH^{gas} and ΔG^{gas} values in kJ/mol of dimer formation reactions. The best by ΔH^{gas} conformers found are shown.

Reactant 1	Reactant 2	Product	DFT		CBS	
			ΔH^{gas}	ΔG^{gas}	ΔH^{gas}	ΔG^{gas}
 Guan (CH_5N_3)	 $AlCl_3$	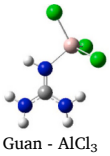 Guan - $AlCl_3$	−207.7	−160.7	−212.5	−165.4
 Urea (CH_4N_2O)	 $AlCl_3$	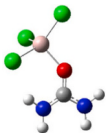 Urea - $AlCl_3$	−171.4	−124.9	−181.4	−134.9

Table 3
The calculated Boltzmann averaged ΔH^{gas} and ΔG^{gas} values in kJ/mol of trimer formation reactions. The best by ΔH^{gas} conformers found are shown.

Reactant 1	Reactant 2	Product	DFT		CBS	
			ΔH^{gas}	ΔG^{gas}	ΔH^{gas}	ΔG^{gas}
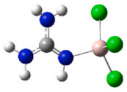 Guan - $AlCl_3$	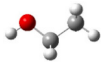 C_2H_5OH (ethanol)	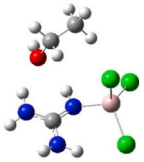 Guan - $AlCl_3$ - C_2H_5OH	−54.0	−3.2	−47.0	3.7
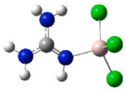 Guan - $AlCl_3$	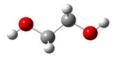 $C_2H_6O_2$ (ethylene glycol)	 Guan - $AlCl_3$ - $C_2H_6O_2$	−74.8	−19.0	−64.7	−9.1
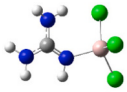 Guan - $AlCl_3$	 C_2H_6O (dimethyl ether)	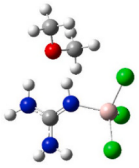 Guan - $AlCl_3$ - C_2H_6O	−48.7	−2.1	−43.8	2.7
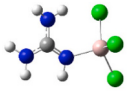 Guan - $AlCl_3$	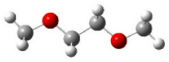 $C_4H_{10}O_2$ (1,2-dimethoxyethane)	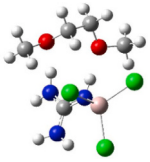 Guan - $AlCl_3$ - $C_4H_{10}O_2$	−75.1	−18.6	−66.3	−9.8

interaction with the nearest atoms is considered admittedly accurately. In addition, if we compare full-sized molecules, the entropy factor will be approximately the same, since the influence of the functional groups of radicals H-O-C- / -C-O-C- will be insignificant based on the ratio of their number of several units per several thousand atoms in the complete chain of the molecule, while the enthalpy will be noticeably different and have approximate values to the model taken in this study.

The reaction of Guan and $AlCl_3$ was primarily investigated (as well as comparison with the reaction of Urea and $AlCl_3$). The computational results are presented in Table 2. In the best conformer of Guan-$AlCl_3$ complex, the non-covalent intermolecular interaction Al-N is more favorable with the nitrogen atom bonded to only one hydrogen (Table 2). In case of Urea-$AlCl_3$ complex, the interaction between Al-O is more favorable in terms of thermodynamics, which has also been noted by other authors [17]. The enthalpy of interaction between Guan and $AlCl_3$ is by about −35 kJ/mol lower than between Urea and $AlCl_3$, which is to be expected given that the oxygen atom is more electronegative than the nitrogen. This also indicates that the Guan molecule is a better Lewis base (better electron donor) than the Urea molecule.

Molecules of ethanol, ethylene glycol, dimethyl ether, and 1,2-

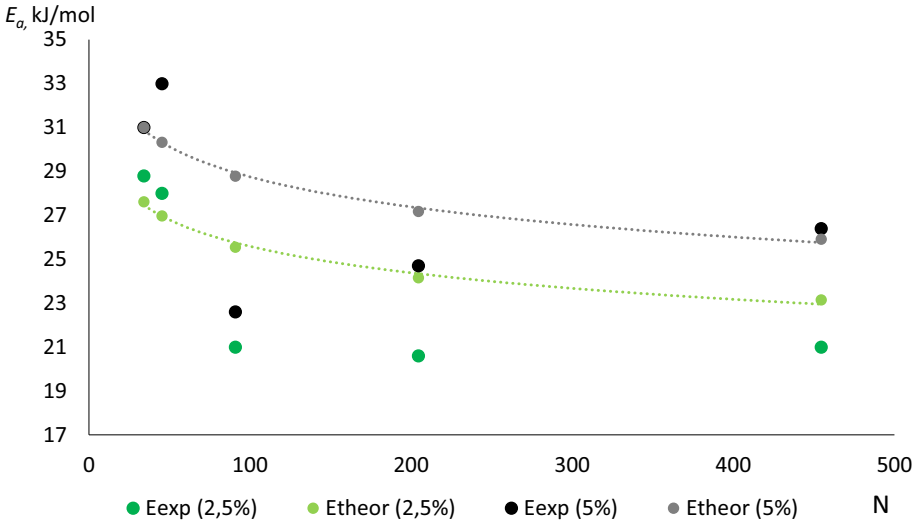

Fig. 5. The graphic representation of the fitting results for activation energy values N (the number of subunits, defined in the text).

dimethoxyethane were used as a model of solvent-fragment (oligomer) interacting with Guan-$AlCl_3$ complex. We found that in all studied Guan-$AlCl_3$-oligomer complexes, in their best conformers, oligomer tends to form intermolecular hydrogen bonds of the N-H…O type with the Guan molecule. Hydrogen bonds of the same type were observed by the authors [17] when modeling complexes with Urea molecules.

When going from ethanol to ethylene glycol, the effect of the second oxygen is visible and the enthalpy of trimer formation decreases, because in the Guan-AlCl3-$C_2H_6O_2$ complex energetically more favorable intermolecular hydrogen bonds are formed between the oligomer and Guan. The same effect is observed when moving from dimethyl ether to 1,2-dimethoxyethane. That is, instead of forming two hydrogen bonds with one oxygen atom of the N_{amino}-H…O…H-N_{imino} type, the most energetically preferable would be the formation of two hydrogen bonds: one for each oxygen atom of the N_{amino}-H…O type and N_{imino}-H…O.

Comparing the calculated energies of formation of complexes with such oligomers as ethanol and dimethyl ether, we see that the interaction energy weakly depends on which oxygen atom hydrogen bonds are formed with: with oxygen of the hydroxy group or with ether oxygen. This is also true for ethylene glycol and 1,2-dimethoxyethane.

The direct comparison with experimental data analysis in Fig. 5 should be done using ethanol (entry 1) and dimethyl ether (entry 3) which contains single oxygen. Second oxygen gives an artifact of bunding to both of them. The DFT calculation gives binding enthalpies −58.8 and −53.9 kJ/mol for ethanol and dimethyl ether respectively, while the CBS method gives −46.8 and −43.8 kJ/mol. Experimental values are for activation energies being correspondingly 34.4, 21.9 kJ/mol for 2.5 % PEO and for 5 % concentration 37.9, 24.0 kJ/mol for E_{end} and E_{mid}. Now, the “end” position should be associated with ethanol (entry 1) whereas the “mid” one the emulated by dimethyl ether. The difference in the calculated enthalpies is 3–5 kJ/mol, whereas activation energies are shifted by 13 kJ/mol. The sign is correct, so the absolute value is not, albeit by reasonable margin for simplicity of treatment both of experimental data and modeling.

Comparing with $AlCl_3$-urea-PEO [16,17] and $AlCl_3$-Emim-PEO [15] current system behaves as elastomer, or the former. Emim system and solidifies due to 5 coordinated Al [15]. Correspondingly our DFT model resembles more used in [17].

Finally, PEO 2000 with both methyl at the ends has lower activation energies. Though to analyze better this result one needs more data with different molecular weights.

8. Conclusions

It was found in this study that the addition of polymer macromolecules affects the structure of the electrolyte in the system with GuanHCl-$AlCl_3$ complex. The activation energy (E_a) values were calculated for a GuanHCl-$AlCl_3$ system with PEG additives of various molecular weights (from 1500 to 5 million). Quantum-chemical computation showed a difference in the values of enthalpy (ΔH^{gas}) or Gibbs free energy (ΔG^{gas}) in the formation of a complex both between of Guan and $AlCl_3$ as well as comparison with the reaction of urea and $AlCl_3$, and comparison of Guan-$AlCl_3$ with various functional groups of polymers. It can be concluded, that the internal resistance of the electrolyte decreases with an increase in the molecular weight of the added polymer (such as polymer macromolecules), in the concentration range from 2.5 to 10 % (which is confirmed by the minimum value of the activation energy in a certain area). The method presented in this paper is related to the measurement of the temperature dependence of the ionic conductivity of electrolytes for polymers with different chain lengths. Further from the indicated Arrhenius law is the activation energy, which determines the contribution of the functional groups located in the polymer chain, as well as the terminal functional groups. Polymer with longer chain has more low energy binding sites which causes lesser binding and consequently higher conductivity of electrolyte. As a result of the conducted research, the experimental data have been obtained that determine unexpected conclusions about the nature of the processes. It is planned to conduct further research to clarify the patterns in model systems - electrolytes of a similar nature, for example acetamidine, with additives of the corresponding polymers.

Computational analysis revealed that the Guan-$AlCl_3$ complex exhibited a more favorable interaction compared to Urea-$AlCl_3$, indicating Guan’s superior Lewis basicity. The study extended to Guan-$AlCl_3$ complexes with solvent-fragment oligomers, highlighting the impact of additional oxygen atoms on the energetics of trimer formation. Interestingly, the calculated energies showed a weak dependence on the specific oxygen atom involved, emphasizing the versatility of the interactions studied across different oligomers. Overall, these findings contribute to a deeper understanding of the molecular interactions involved in these systems.

CRediT authorship contribution statement

Roman Tangalychev: Writing – original draft, Investigation, Formal analysis, Data curation. **Vasilii Korotenko:** Writing – original draft, Investigation, Formal analysis. **Igor Efimov:** Writing – review & editing, Formal analysis, Conceptualization. **Oleg N. Efimov:** Methodology, Conceptualization.

Declaration of competing interest

The authors declare the following financial interests/personal relationships which may be considered as potential competing interests:

Igor Efimov reports financial support was provided by Alexander von Humboldt Foundation. If there are other authors, they declare that they have no known competing financial interests or personal relationships that could have appeared to influence the work reported in this paper.

Data availability

Data will be made available on request.

Acknowledgements

The authors are grateful to Prof. A. Bund and Dr. A. Ispas for generous providing of laboratory equipment and chemicals in TU Ilmenau, where the work was carried out, and for stimulating discussions and early reading of manuscript. IE thanks A. von Humboldt Foundation for research grant. We gratefully acknowledge Leibniz-Rechenzentrum (LRZ) in Munich for providing the computational resources and software.

References

[1] H. Zhang, L. Qiao, H. Kühnle, E. Figgemeier, M. Armand, G.G. Eshetu, From lithium to emerging mono-and multivalent-cation-based rechargeable batteries: non-aqueous organic electrolyte and interphase perspectives, Energ. Environ. Sci. 16 (1) (2023) 11–52.
[2] B. Craig, T. Schoetz, A. Cruden, C.P. de Leon, Review of current progress in non-aqueous aluminium batteries, Renew. Sustain. Energy Rev. 133 (2020) 110100–110117.
[3] M.-C. Lin, M. Gong, B. Lu, Y. Wu, D.-Y. Wang, M. Guan, M. Angell, C. Chen, J. Yang, B.-J. Hwang, An ultrafast rechargeable aluminium-ion battery, Nature 520 (7547) (2015) 324–328.
[4] D.-Y. Wang, C.-Y. Wei, M.-C. Lin, C.-J. Pan, H.-L. Chou, H.-A. Chen, M. Gong, Y. Wu, C. Yuan, M. Angell, Advanced rechargeable aluminium ion battery with a high-quality natural graphite cathode, Nat. Commun. 8 (1) (2017) 14283–14290.
[5] T.-L. Hsieh, C.-T. Tsai, M.-C. Lin, An acetamidine-based gel polymer electrolyte assists durable rechargeable aluminum/graphite cells, Graphite Cells.
[6] H. Sun, W. Wang, Z. Yu, Y. Yuan, S. Wang, S. Jiao, A new aluminium-ion battery with high voltage, high safety and low cost, Chem. Commun. 51 (59) (2015) 11892–11895.
[7] R. Böttcher, S. Mai, A. Ispas, A. Bund, Aluminum deposition and dissolution in [emim] Cl-based ionic liquids–kinetics of charge–transfer and the rate–determining step, J. Electrochem. Soc. 167 (10) (2020) 102516–102525.

[8] T. Schoetz, J.H. Xu, R.J. Messinger, Ionic liquid electrolytes with mixed organic cations for low-temperature rechargeable aluminum–graphite batteries, ACS Appl. Energy Mater. 6 (5) (2023) 2845–2854.
[9] H. Jiao, C. Wang, J. Tu, D. Tian, S. Jiao, A rechargeable Al-ion battery: Al/molten AlCl 3–urea/graphite, Chem. Commun. 53 (15) (2017) 2331–2334.
[10] D. Paterno, E. Rock, A. Forbes, R. Iqbal, N. Mohammad, S. Suarez, Aluminum ions speciation and transport in acidic deep eutectic AlCl3 amide electrolytes, J. Mol. Liq. 319 (2020) 114118–114146.
[11] A.V. Borozdin, P.Y. Shevelin, V.A. Elterman, L.A. Yolshina, Electrochemical behavior of aluminum in triethylamine hydrochloride–aluminum chloride ionic liquid, PCCP 25 (44) (2023) 30543–30552.
[12] A.J. Lucio, I. Efimov, O.N. Efimov, C.J. Zaleski, S. Viles, B.B. Ignatiuk, A.P. Abbott, A.R. Hillman, K.S. Ryder, Amidine-based ionic liquid analogues with AlCl 3: a credible new electrolyte for rechargeable Al batteries, Chem. Commun. 57 (77) (2021) 9834–9837.
[13] R.G. Pearson, Hard and soft acids and bases, J. Am. Chem. Soc. 85 (22) (1963) 3533–3539.
[14] I. Sumarlan, A. Kunverji, A.J. Lucio, A.R. Hillman, K.S. Ryder, Comparative study of guanidine-, acetamidine-and urea-based chloroaluminate electrolytes for an aluminum battery, J. Phys. Chem. 127 (38) (2023) 18891–18901.
[15] T. Schoetz, O. Leung, C.P. de Leon, C. Zaleski, I. Efimov, Aluminium deposition in EMImCl-AlCl3 ionic liquid and ionogel for improved aluminium batteries, J. Electrochem. Soc. 167 (4) (2020) 040516–040528.
[16] Á. Miguel, N. García, V. Gregorio, A. López-Cudero, P. Tiemblo, Tough polymer gel electrolytes for aluminum secondary batteries based on urea: AlCl3, prepared by a new solvent-free and scalable procedure, Polymers 12 (6) (2020) 1336–1350.
[17] Á. Miguel, R.P. Fornari, N. García, A. Bhowmik, D. Carrasco-Busturia, J.M. García-Lastra, P. Tiemblo, Understanding the molecular structure of the elastic and thermoreversible AlCl3: urea/polyethylene oxide gel electrolyte, ChemSusChem 13 (20) (2020) 5523–5530.
[18] O.M. Leung, L.W. Gordon, R.J. Messinger, T. Prodromakis, J.A. Wharton, C. Ponce de León, T. Schoetz, Solid polymer electrolytes with enhanced electrochemical stability for high-capacity aluminum batteries, Adv. Energy Mater. 14 (8) (2024) 2303285–2303296.
[19] A.J. Lucio, I. Sumarlan, E. Bulmer, I. Efimov, S. Viles, A.R. Hillman, C.J. Zaleski, K. S. Ryder, Measuring and enhancing the ionic conductivity of chloroaluminate electrolytes for Al-ion batteries, J. Phys. Chem. 127 (28) (2023) 13866–13876.
[20] A.P. Abbott, R.C. Harris, Y.-T. Hsieh, K.S. Ryder, I.-W. Sun, Aluminium electrodeposition under ambient conditions, PCCP 16 (28) (2014) 14675–14681.
[21] M. Frisch, G. Trucks, H.B. Schlegel, G.E. Scuseria, M.A. Robb, J.R. Cheeseman, G. Scalmani, V. Barone, B. Mennucci, G. Petersson, Gaussian 09, Revision d. 01, Gaussian, Inc., Wallingford CT 201, 2009.
[22] D. Šakić, M. Hanževački, D.M. Smith, V. Vrček, A computational study of the chlorination and hydroxylation of amines by hypochlorous acid, Org. Biomol. Chem. 13 (48) (2015) 11740–11752.
[23] D. Šakić, Kick. https://github.com/DSakicLab/kick/tree/master/, 2024. Accessed in January 2024.
[24] A.D. Becke, Density-functional thermochemistry. I., The effect of the exchange-only gradient correction, J. Chem. Phys. 96 (3) (1992) 2155–2160.
[25] C. Lee, W. Yang, R.G. Parr, Development of the Colle-Salvetti correlation-energy formula into a functional of the electron density, Phys. Rev. B 37 (2) (1988) 785–789.
[26] S. Grimme, J. Antony, S. Ehrlich, H. Krieg, A consistent and accurate ab initio parametrization of density functional dispersion correction (DFT-D) for the 94 elements H-Pu, J. Chem. Phys. 132 (15) (2010) 154104–154124.
[27] W.J. Hehre, R. Ditchfield, J.A. Pople, Self—consistent molecular orbital methods. XII. Further extensions of Gaussian—type basis sets for use in molecular orbital studies of organic molecules, J. Chem. Phys. 56 (5) (1972) 2257–2261.
[28] R.F. Ribeiro, A.V. Marenich, C.J. Cramer, D.G. Truhlar, Use of solution-phase vibrational frequencies in continuum models for the free energy of solvation, J. Phys. Chem. 115 (49) (2011) 14556–14562.
[29] V. Korotenko, H. Zipse, The stability of oxygen-centered radicals and its response to hydrogen bonding interactions, J. Comput. Chem. 45 (2) (2024) 101–114.
[30] V. Korotenko, Energy Sorting Script. https://github.com/vnkorotenko/ess, 2022. Accessed in January 2024.
[31] V. Korotenko, Centroid Comparison Script. https://github.com/vnkorotenko/ccs, 2022. Accessed in January 2024.
[32] M. Balkenhohl, H. Jangra, I.S. Makarov, S.M. Yang, H. Zipse, P. Knochel, A predictive model towards site-selective metalations of functionalized heterocycles, arenes, olefins, and alkanes using TMPZnCl·LiCl, Angew. Chem. Int. Ed. 59 (35) (2020) 14992–14999.
[33] S. Kumar Rout, A. Kastrati, H. Jangra, K. Schwärzer, A.S. Sunagatullina, M. Garny, F. Lima, C.E. Brocklehurst, K. Karaghiosoff, H. Zipse, Reliable functionalization of 5, 6-fused bicyclic N-heterocycles pyrazolopyrimidines and imidazopyridazines via zinc and magnesium organometallics, Chem. A Eur. J. 28 (33) (2022) 1–10.
[34] A. Kastrati, A. Kremsmair, A.S. Sunagatullina, V. Korotenko, Y.C. Guersoy, S. K. Rout, F. Lima, C.E. Brocklehurst, K. Karaghiosoff, H. Zipse, Calculation-assisted regioselective functionalization of the imidazo [1, 2-a] pyrazine scaffold via zinc and magnesium organometallic intermediates, Chem. Sci. 14 (40) (2023) 11261–11266.
[35] A. Altun, F. Neese, G. Bistoni, Local energy decomposition analysis of hydrogen-bonded dimers within a domain-based pair natural orbital coupled cluster study, Beilstein J. Org. Chem. 14 (2018) 919–929.
[36] M. Saitow, U. Becker, C. Riplinger, E.F. Valeev, F. Neese, A new near-linear scaling, efficient and accurate, open-shell domain-based local pair natural orbital coupled cluster singles and doubles theory, J. Chem. Phys. 146 (16) (2017) 164105–164137.
[37] F. Neese, Software update: the ORCA program system, version 4.0, Wiley Interdiscip, Rev. Comput. Mol. Sci. 8 (1) (2018) e1327.
[38] F. Neese, E.F. Valeev, Revisiting the atomic natural orbital approach for basis sets: robust systematic basis sets for explicitly correlated and conventional correlated ab initio methods? J. Chem. Theory Comput. 7 (1) (2011) 33–43.